OPTICAL DESIGN OF THE PROTON BEAMLINES FOR THE PROSCAN PROJECT

U. Rohrer

The optical design for the final layout of the beam lines for the PROSCAN project is presented here. Optical computations were mainly done in 1st order for the basic design and additionally up to 3rd order to study also the influence of contributions to the beam due to chromatic aberrations. Similar work for the design of the Gantries and the Optis apparatus is done by ASM and covered by contributions elsewhere.

INTRODUCTION

Since 1999 design studies have been under way for finding a location in the former NA-hall to place the new 250 MeV Proscan cyclotron (COMET). It has to deliver its produced proton beam to an already existing and 3 new areas for biomedical applications (as well as a proton irradiation facility PIF). Some of the many different preliminary versions are shown in references [1] and [2]. A simplified view of the Proscan beam lines for today's practically finalized floor plan layout is shown in Fig. 1. Only the most important components like cyclotron, kicker magnet, degrader, collimator, momentum slits, 7 bending magnets, 44 quadrupole lenses, meeting points (UP) and beam axes are drawn.

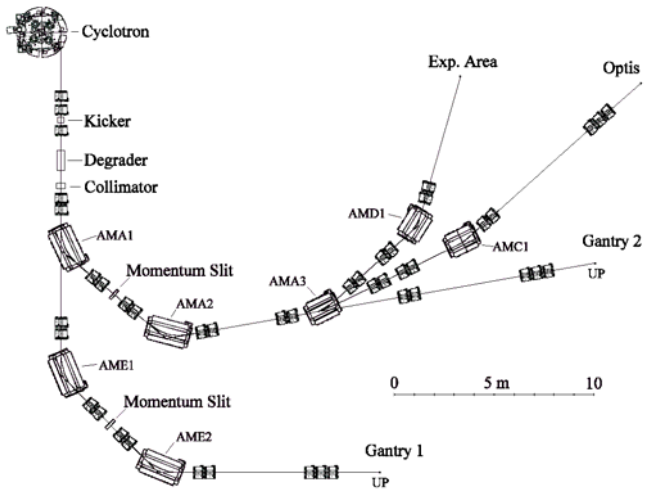

Fig. 1: Floor plan layout of the 4 Proscan beam lines to Gantry1, Gantry2, Optis and the Experimental Area. Included are only the main optical components.

DIVISION IN GROUPS

The optical design of the beam lines may best be done by dividing the problem into 5 different sections:

(1) cyclotron exit → degrader (Fig. 2)
(2) degrader → UP of Gantry 1 (Fig. 3)
(3) degrader → UP of Gantry 2
(4) degrader → Optis area (UP not yet defined)
(5) degrader → experimental area (e.g. for PIF).

Since the space for this article is limited the detailed discussion will cover only the sections 1 and 2. Because the same criteria were applied for all cases, the optical design for sections 3 to 5 look pretty similar to the one for section 2, which will be discussed here in more details.

COMMON SECTION WITH DEGRADER

Results of TRANSPORT [4] calculations done for beam line section 1 are shown in Fig 2. With the first Q-triplet after the cyclotron, a beam spot as small as possible is produced at the degrader consisting of high-density (ρ=1.88 g/cm^3) graphite wedges [3]. In order to get a round spot at the degrader – which is desirable – the projected emittances in x and y have to be equal within about a factor of 2 (not yet the case with the latest cyclotron model calculations done by Accel, Fig. 2). A fast kicker magnet (5 mrad horizontal deflection-angle) for on/off-switching the beam on user request (within 100 μs) is mounted between the 2nd and 3rd quadrupole lens. Because the 3rd lens is horizontally defocusing, the deflection of the centroid is amplified by a factor of 1.5, which results in a horizontal beam deviation from the axis of about 12 mm at the stopper located near the entrance of the degrader box [3]. First Monte-Carlo simulations with the computer code TURTLE [5] show that under ideal conditions beam suppression ratios down to 10^{-5} should be reachable with the kicker.

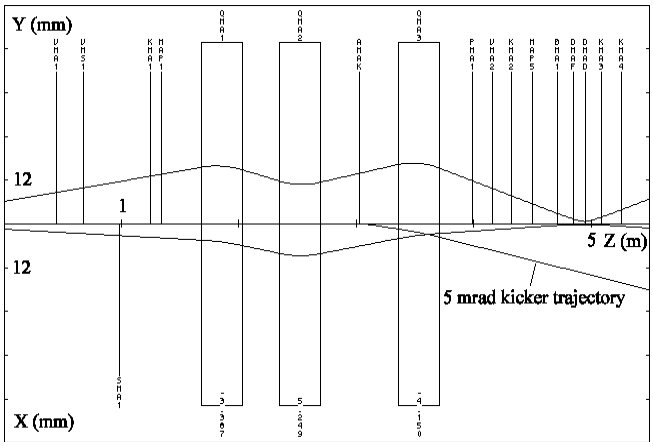

Fig. 2: First order 2σ-envelopes of the beam starting at the cyclotron exit and going through the first Q-triplet to the degrader together with the central trajectory of the beam horizontally deflected by the kicker magnet. The used values of the projected emittances ε_x=0.65π mmmrad and ε_y=10.3π mmmrad are from preliminary data delivered by Accel (manufacturing company of the 250 MeV cyclotron).

BEAM LINE TO GANTRY 1

Fig. 3 shows the 1st and 2nd order Transport envelopes of the optics for the beam line section between the virtual waist in the degrader and the meeting point of Gantry 1 (UP).

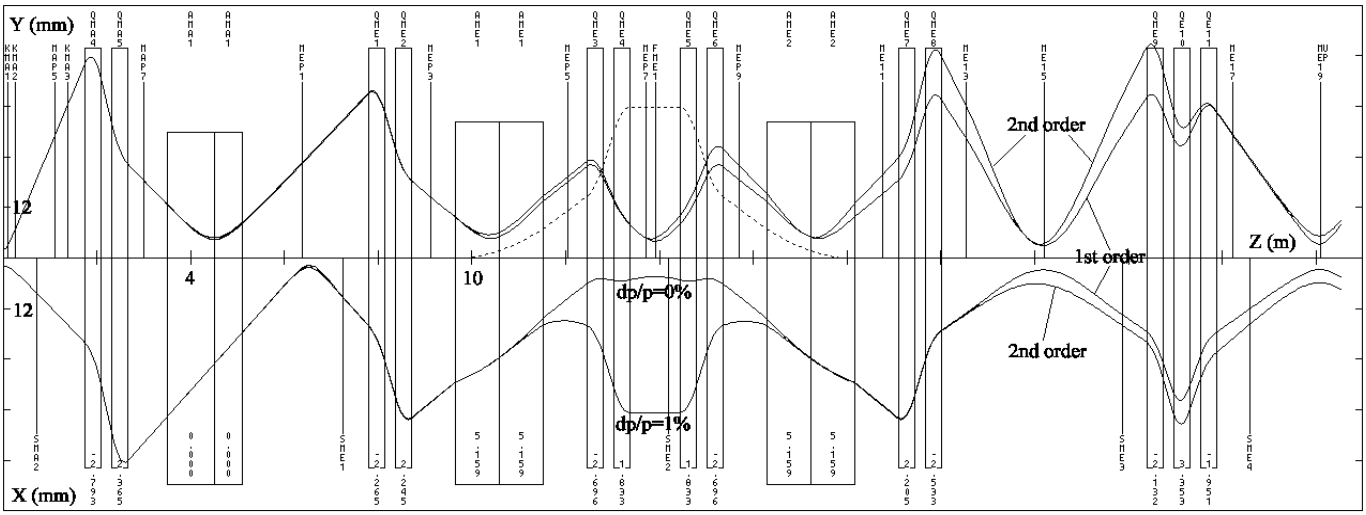

Fig. 3: First and second order envelopes of the 70 MeV-optics for the beam line between the degrader and the meeting point of the existing Gantry 1. The dotted line is the 1%-dispersion trajectory. At the dispersive focus both envelopes for dp/p=0 % and 1 % are drawn. The second order contributions are mainly caused by the chromatic aberration-coefficients T126 and T346 (Fig. 4).

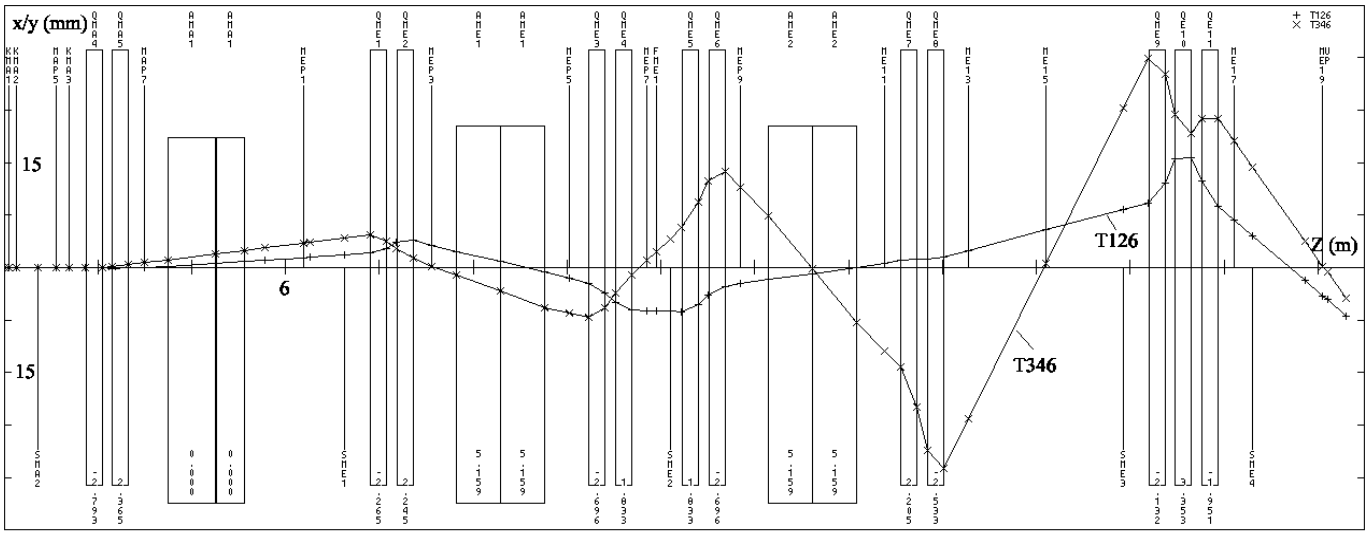

Fig. 4: The 2 beam-contributions from the 2nd order chromatic aberration-coefficients T126 and T346. (In this graphic display the contribution to the envelopes of both coefficients is drawn for dp/p=1 % and x_0'=11.6 mrad or y_0'=26.6 mrad.)

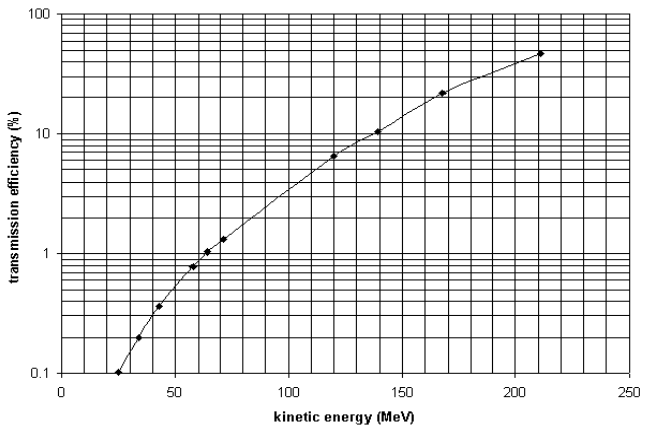

Fig. 5: Transmission efficiency of the Proscan beam lines as a function of the kinetic energy. At 70 MeV the value for the transmission is about 1.3 ± 0.1 %.

As x- and y-starting values 2 mm are used, whereas the x'- and y'-starting values are chosen to display the maximum amplitudes allowed to be inside the quadrupole apertures (x_0'= 11.6 mrad and y_0'=26.6 mrad). All of them have an aperture radius of 50 mm and the inside diameters of the vacuum tubes are 90 mm. A vertical waist is placed in all 3 bending magnets so that a gap size of 65 mm is sufficient (inside height of vacuum chamber = 54 mm). Two bending magnets (AME1 and AME2) and 4 symmetrically arranged quadrupoles are needed to deflect the beam by 90 degrees and to keep under control the dispersion and the vertical cosine-trajectory. At the intermediate focus between the 2 Q-duplets the momentum bandwidth may be controlled by a movable slit-collimator. In this region both horizontal envelopes for dp/p=0 % and 1 % together with the dotted 1%-dispersion trajectory are drawn.

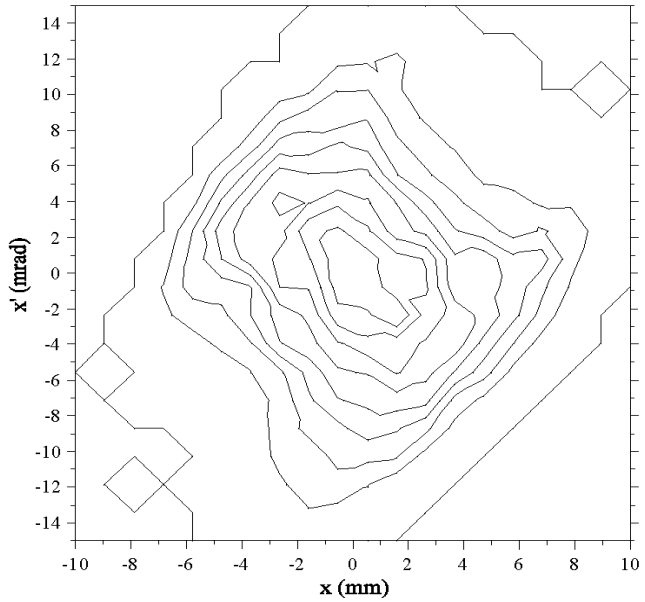

Fig. 6: x/x'-contour diagram of a Monte-Carlo first-order simulation for the 70 MeV beam at the meeting point (UP) for Gantry 1. The RMS-value for x is 2.9 mm and for x' 4.7 mrad.

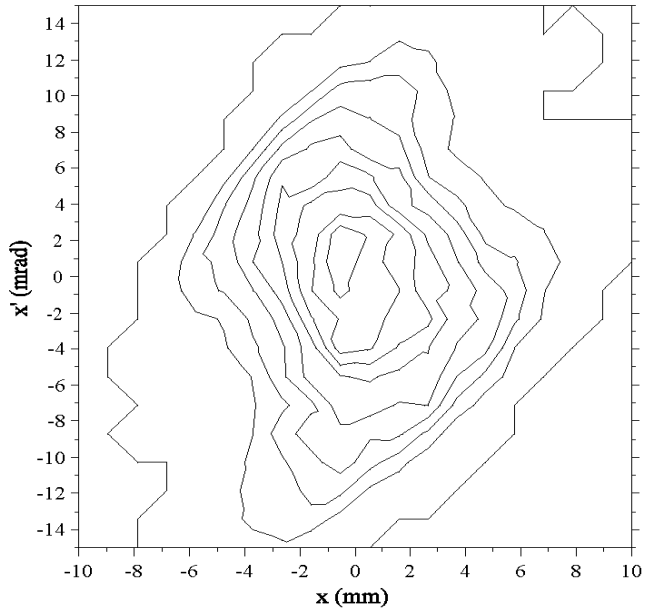

Fig. 7: x/x'-contour diagram of a Monte-Carlo third-order simulation for the 70 MeV beam at the meeting point (UP) for Gantry 1. The RMS-value for x is 2.6 mm and for x' 5.3 mrad.

HIGHER ORDER EFFECTS

The display of the second half of this beam line section (Fig. 3) shows a well visible difference between the 1st and 2nd order envelopes. The dominant 2nd-order contributions are due to the chromatic aberration-coefficients T126 and T346. These 2 coefficients are graphically displayed in Fig. 4 for a dp/p = 1 %, x_0'= 11.6 mrad and y_0' = 26.6 mrad. According to the magnitude of the 2nd-order effects at the meeting-point (UP), the beam spot size would almost double compared with the 1st-order values, which would require, that some sextupole correcting devices may have to be inserted into the beam line. But a Monte-Carlo simulation with the computer-code TURTLE [5] shows, that this is not necessary. Fig. 6 and Fig. 7 show the x/x'-contour-plot at the meeting point UP of Gantry 1. There is almost no significant difference between the 1st-order only and the one, which shows the results of computations with contributions of up to 3rd-order. This effect has also been observed at PSI's high-acceptance muon beam lines [6], where tests with the real beam show, that the TRANSPORT 2nd-order envelopes are overestimated and that the results of TURTLE computations correspond pretty much to the measured beam spots.

SPECIAL DEVICES

For the verification of the optics and for centring the proton beam along the beam line, a series of beam scanners (profile monitors) for both directions (in x and y) are required. In Fig. 3 (and Fig. 4) the position of these devices are marked with vertical lines pointing upwards and having labels like MAnn/MEnn. The positions of the steering magnets required for centring the beam are marked similarly with vertical lines pointing downwards and having labels like SMAn/SMEn. All quadrupole lenses are equipped with mirror plates in order to avoid overlapping effects with the fringe fields of the adjacent quadrupoles. This helps to produce a good agreement of measured beam envelope with TRANSPORT predictions, because the effective lengths of the quadrupoles remain uninfluenced by their actual settings. As may be seen from Fig. 3 and Fig. 9 some beam losses will occur at all quadrupoles. Therefore after each Q-duplet and Q-triplet a 4-segment halo monitor will be placed to gather some information about the beam spill for an online display.

MEETING POINT CONDITIONS

Fig. 7 gives also the 1σ-values of x and x' at the meeting point UP of Gantry 1. Since a Q-triplet is used in front of the meeting point (UP), it is possible to tune its settings in such a way, that a 'round' (x=y) spot at the UP may be achieved. Thus, for the reason of a good matching with the Gantry 1 optics at UP [2], the 2σ-values of the projected emittance at the double-waist listed below are met.

$$x \approx y \approx 6 \text{ mm} \quad \text{and} \quad x' \approx y' \approx 10 \text{ mrad}$$

Because for the three other beam line sections similar optical device blocks are used, no significant differences in the optical design are apparent and worthwhile to be mentioned or shown in this article.

TRANSMISSION EFFICENCY

The transmission efficiency of the beam lines to the Gantries and the Optis and Experimental areas is strongly dependent on the chosen kinetic energy of the protons (Fig. 5). This is due to the fact, that the energy and angular straggling of the degrader material with variable thickness are producing a phas-espace that can be larger than the phase space acceptance of the beam lines. The dp/p-distribution of

the accepted and transmitted protons is shown in Fig. 8. Its width is about ±1.2 %, which is given by the dispersion trajectory between AME1 and AME2 and the aperture size there (Fig. 3). This maximum value is considered to be sufficient for the production of a smooth SOBP (Spread-Out-Bragg-Peak) with not too many energy steps [2].

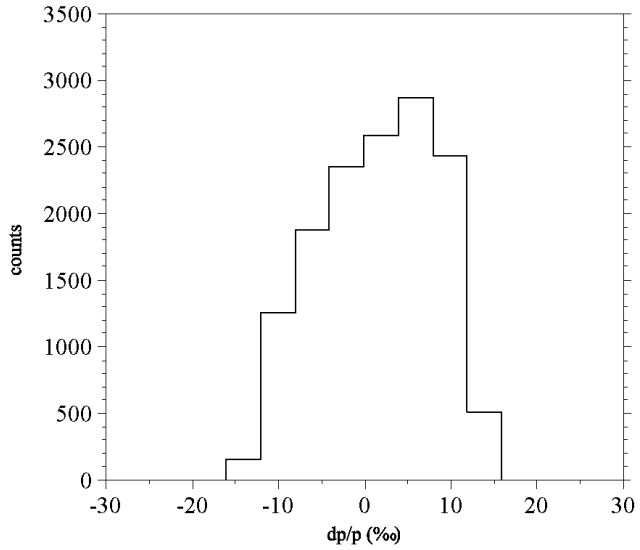

Fig. 8: Momentum transmission distribution of the Proscan beam lines (at 70 MeV). The RMS-value is about 0.68 %.

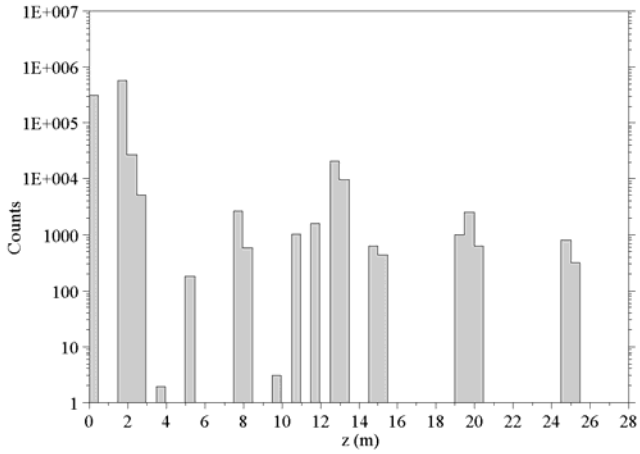

Fig. 9: Result of a Monte-Carlo simulation (3rd order) of the losses for protons along the beam line between the degrader (z = 0 m) and the meeting point (UP at z ≈ 28 m) of Gantry 1 for E = 70 MeV beam-settings. The location of the components along z may be seen from Fig. 4.

BEAM LOSSES

For almost all energies used for proton therapy the degrader has to be used. Therefore the full aperture of all quadrupoles after the degrader will be filled with some beam, which has the consequence, that at each Q-duplet or Q-triplet some protons will be lost. Fig. 9 shows a typical loss diagram (computed with the Monte-Carlo program TURTLE [5]) along the beam line from the degrader to the Gantry 1 meeting point with a longitudinal resolution of 0.5 m. The used model is simplified by only applying multiple scattering at the degrader and not at the following aperture constraints. In reality the losses will be more smeared out. In this example the degrader was set for degrading the proton beam from 250 down to 70 MeV (kinetic energy) and the number of tracked particles was 10^6 protons. Most of them (95 %) are lost at the degrader and the following (x'/y')-definition-slit in front of the 1st Q-duplet. Therefore, starting at the degrader the first 3 to 4 metres of the beam line are becoming the most activated region of the PROSCAN beam lines. Some local shielding for the components here has to be foreseen. The sum of the lost protons along the whole beam line at 70 MeV is 98.5 % in a 1st-order run and 0.06 % higher in a 3rd-order run, since there are slightly more protons with exceeding amplitude in the last Q-duplet and Q-triplet (Fig. 3).

FINAL REMARKS

If the reader would like to learn more about the PROSCAN beam lines in a wider context, then the review document "Architectural overview of the PROSCAN beam lines" compiled by M. Schippers [7] is recommended to be looked at. To further confirm the claim, that higher order aberrations are not influencing the beam transport substantially, it is planned to study the optical behaviour of the current layout also with the computer code COSY INFINITY [8].

REFERENCES

[1] H. Reist et al., *Project Study for Proscan,* PSI Scientific and Technical Report 1999, VI, p. 22-23.

[2] E. Pedroni, *Spezifikationen für PROSCAN aus der Sicht des Benützers*, Review Document B, P00/PE21-071.0, version 2-Oct-2000.

[3] H. Reist et al., *A Fast Degrader to set the Energies for the Application of the Depth Dose in Proton Therapy*, PSI Scientific and Technical Report 2001, VI, p. 20-21.

[4] U. Rohrer, *Graphic Transport*, downloadable code with some online documentation via the web, http://people.web.psi.ch/rohrer_u/trans.htm

[5] U. Rohrer, *Graphic Turtle*, downloadable code with some online documentation via the web, http://people.web.psi.ch/rohrer_u/turtle.htm

[6] D. Renker, private communication.

[7] M. Schippers, *Architectural overview of the PROSCAN beam lines*, Review Document F, P00/SJ85-109.2, version 15 November 2002.

[8] M. Berz, *COSY INFINITY*, an arbitrary order beam dynamics simulation and analysis code, downloadable via the web from the Department of Physics and Astronomy at the Michigan State University, see http://cosy.pa.msu.edu/

[4] F. Atchison, Some results from neutronic-calculations of the D_2 cold-neutron source, SINQ project report SINQ/816/AF38-901 (1989).